Journal of Hydroscience and Hydraulic Engineering
Vol. 17, No.2 November, 1999, 59-70

FLOW PROPERTIES OF A DEEP OPEN EXPERIMENTAL CHANNEL WITH A DENSE VEGETATION BANK

By

Kazuyoshi HASEGAWA
Div. of Civil and Environmental Engineering, Hokkaido University, Sapporo, Japan
Shigemasa ASAI
Tokyo Metropolitan Government, Tokyo, Japan
and
Shugo KANETAKA and *Hitoshi* BABA
Civil Engineering Research Institute, Hokkaido Development Bureau, Sapporo, Japan

SYNOPSIS

A characteristic flow velocity field was examined in a deep open experimental channel having one side bank covered with dense model plants. A vertical profile of the main flow velocity showed a convex shape with a maximum velocity at one-third of the water depth from the bottom. The velocity gradually decreased towards the water surface and the bottom. Reynolds stress was negative in two-thirds of the water column; cross-sectional secondary flows were generated near the bank vegetation. These flows possibly originated from generation of strong boils near the bottom of the vegetation boundary. Such flows may transport the fluid mass with a low velocity from the near the bottom to the water surface. Distributions of measured turbulence intensity support this view. From the experimental results, resistance to the mean flow is considered to consist of lateral Reynolds stress caused by the bank vegetation (with about 20% of the share ratio for the resistance force), of lateral momentum transport due to secondary flows (with about 30%), and of bed shear stress (with about 50%).

INTRODUCTION

Many investigations have elucidated the hydraulic properties of rivers with bank vegetation because of social demands to improve the river environment. Several excellent reviews of such investigations in Japan have been reported (Okabe (5), Ikeda (2), Tsujimoto (7) and Watanabe (9)). These investigations suggest the importance of the following concepts:

(1) Different flow fields appear in a vegetated channel with four different kinds of vegetation as classified from a hydraulic viewpoint: low herb class, high herb class, arbor class and aquatic plant. Particularly, the dimensional features of flow differ depending on if the vegetation is submerged.
(2) The cross-sectional width of vegetative area, the density and permeability of vegetation, channel width and water depth, etc., give important effects on the flow.

(3) Lateral fluid mixing near vegetation boundary has the most important role to produce the boundary shear stress and sediment transport.

Thus, an open channel flow with vegetated banks generally has properties such that the horizontal properties have a greater influence than the other properties. For this reason, almost all hydraulic investigations of vegetated rivers have concentrated on planar two-dimensional problems of flow. When investigating the horizontal velocity distribution and the bed changes in a flow field where lateral momentum mixing develops, the assumption that these phenomena are vertically uniform will naturally be used. Tsujimoto et al (8) confirmed the flatness of the vertical flow profile i.e. the validity of the 2- dimensional flow in an experimental channel with non-submerged thin and regular spaced vegetation.

However, a flow field with a deep water depth in a densely vegetated channel cannot be assumed to have a two-dimensional property, especially when the local flow in the vicinity of the vegetation boundary is taken up. Very few investigations have been made on the three-dimensional structure of flow with vegetation. Only Shimizu et al (6) or Nezu et al (4) have presented results of numerical simulations of three-dimensional flows in a channel with vegetation.

This study aimed to elucidate the effects of stem grass, like reeds, to sustain the surrounding environment and to stabilize the banks. The three-dimensional structures, in particular the vertical change in flow, were positively investigated in this study. For this purpose, a large scale experimental channel of 0.8 m depth and 2 m width with an artificial area of vegetation on the bank was used to investigate the properties of the mean flow distribution, Reynolds stress distribution and turbulent intensities.

OUTLINE OF THE EXPERIMENTS

A concrete channel in the Ishikari River Hydraulics Test Yard of the Civil Engineering Research Institute of Hokkaido Development Bureau (3), 40 m long and 4 m wide, was used for experiments (Fig. 1). Volcanic soil was settled in the channel to form a water channel with one side bank and a bottom (Fig. 1(c)). A conveyer was installed 6 to 7 m downstream from the entrance of the channel to supply the volcanic soil. At the end of the channel, a movable tail gate was installed to control the water surface slope. Many wooden bars were embedded in the bank in the middle reach of channel over 16.1 m and in the width 1.2 m, to act as a vegetation area. Fig. 1(a) is a scene of an experimental channel with the artificial vegetation area. The artificial plants were arranged to be close to a natural state of vegetation; the coordinates of the position of each bar were determined using random numbers as indicated in Figs. 2(a) and 2(b). Two kinds of vegetation density, 1600 reeds /m^2 and 1000 reeds /m^2 (Case1 and Case 2, respectively), were chosen for experiments by referring to the density value of reeds which was known in investigation of the Lake Biwa.

After a preliminary experiment Case 0, that was made with a vegetation density of 1600 reeds /m^2, was carried out, the channel was left for one year in order to stabilize the bank slope, and regular experiments were performed using two kinds of discharge, 0.7 m^3/s and 0.5 m^3/s (Table 1).

In this paper, only experiments using a discharge of 0.7 m^3/s in Case 1 and Case 2 are described and discussed, because the experiment of Case 0 was reported by us previously (1), and because the experiments using larger discharges showed clearer flow properties. The running time was 400 minutes for every case, but the water supply was temporarily stopped after 200 minutes from the start to measure the change in cross sections and longitudinal bed height. Measurements were conducted of the following items:

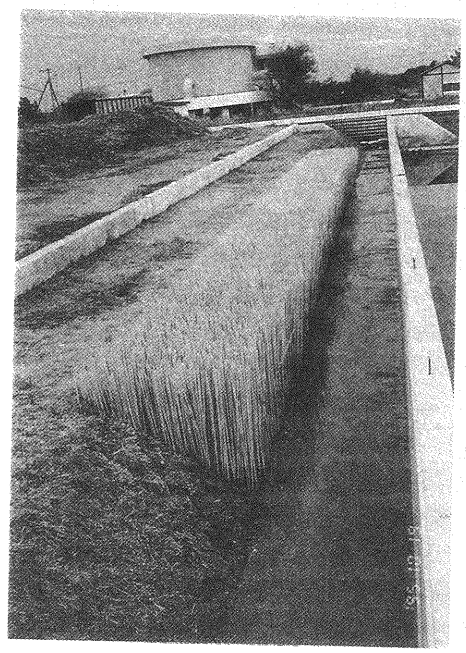

(a)

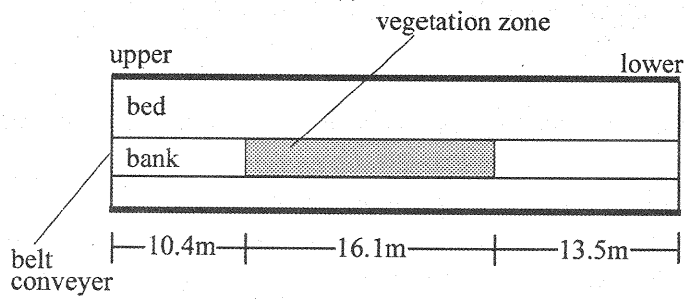

(b)

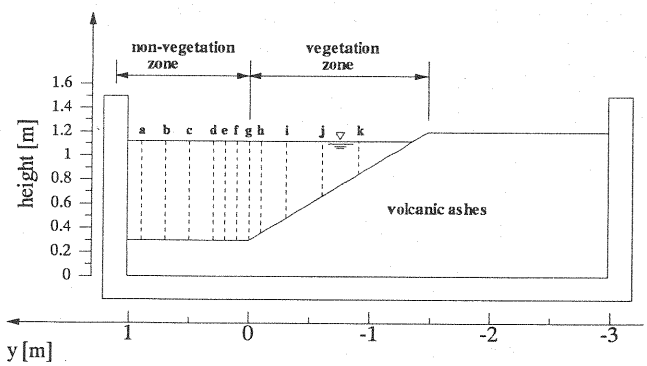

(c)

Fig. 1 Experimental channel, (a) Photo (forward the upstream), (b) Plane view, (c) Cross sectional view.

Table 1 Experimental conditions

Case	Vegetation Density (reeds /m^2)	Initial Bed Gradient	Discharge (m^3/s)	Supplied Sediment Volume (m^3/s)
Case 1	1600	1/1500	0.7	0.028
Case 2	1000	1/1500	0.7	0.028

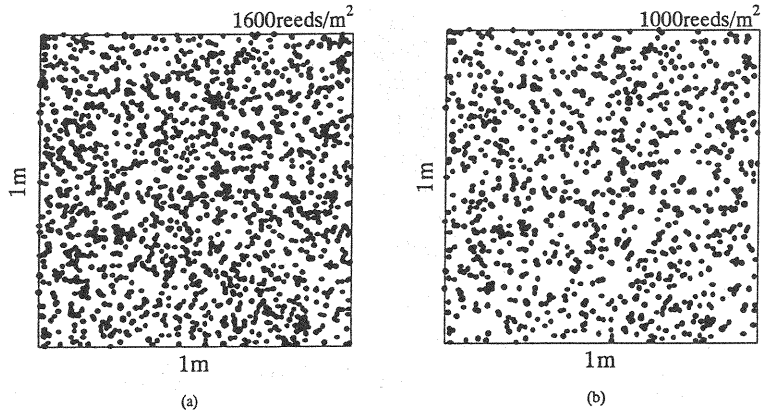

Fig. 2 Channel vegetation densities, (a) Case 1, 1600 reeds/m^2, (b) case 2, 1000 reeds/m^2.

(a) Water surface slope: obtained every 30 minutes after the start of the water running from readings of seven point gauges installed at seven stations 6, 10, 14, 18, 22, 25 and 32 m from the upstream end of the channel along a longitudinal line of 50 cm from the left concrete bank.

(b) Water surface oscillation: measured at 0.5 second intervals using five electric capacity water-gauges installed at five stations 4, 12, 16, 24 and 36 m from the upstream end of the channel along the same longitudinal line of 50 cm from the left concrete bank.

(c) Flow velocity: the mean flow velocities, Reynolds stress distributions and turbulent intensity distributions were measured using a three-dimensional electric magnetic current-meter. The measured points totalled 100 points containing 2 - 11 points in every vertical line of a - k (Fig. 1(c)) arranged in a cross section of 20 m from the upstream end of the channel. At every point, data at 0.1 second intervals of velocity components of the main stream direction, transverse direction and vertical direction were collected during 1 minute. A probe of the current meter was fixed with fishing threads and was pulled in three different directions by reels to prevent inclination and vibration of the rod connected to the probe by the water flow.

(d) Suspended sediment concentration: using water samples collected by using siphon tubes at 41 measuring points to include 6 - 9 points on every vertical line of b, f, h, i and j (Fig. 1(c)) in a cross section 19 m downstream from the upstream end of the channel.

(e) Transversal bed topography: surveyed after drainage and leveling was carried out of the bed height by using an auto-level and a staff gauge, at cross sections 16, 18, 20, 22 and 24 m downstream from the upstream end of the channel.

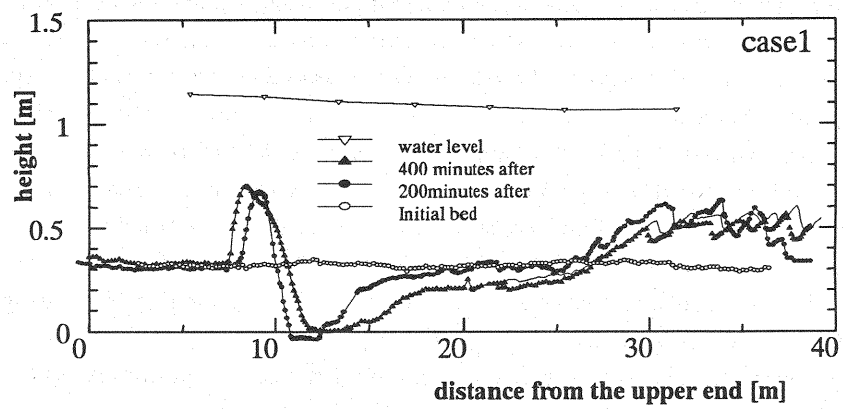

Fig. 3 Longitudinal bed forms at the observation times and water surface height.

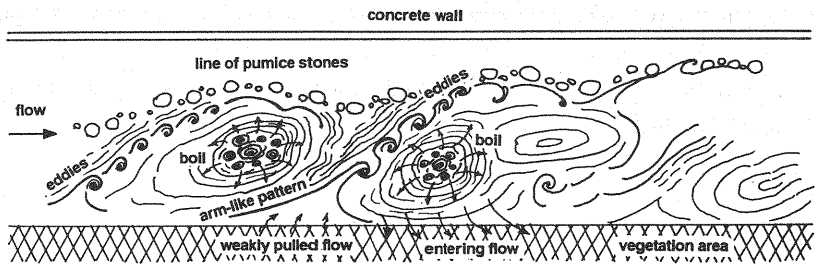

Fig. 4 Sketch of a flow pattern with boils.

(f) Longitudinal bed profile: surveyed after drainage by using an auto-level and a staff gauge along transverse lines 50 cm and 1 m from the left concrete bank.

Hereafter, the artificial model vegetation is called "vegetation". Coordinate measurements were taken along the centerline of the bottom of the concrete channel in the downstream direction for the x-axis, perpendicularly to the x-axis toward the left bank for the y-axis, and vertically upward from the bottom of the concrete channel for the z-axis.

RESULTS

Characteristics of the Flows

Because the vegetation area was constructed partially in the channel (Fig. 1), the entire flow was non-uniform accompanying a suddenly contracted flow and a suddenly expanded flow. Correspondingly, the longitudinal bed profiles showed irregular forms such that the gradients became negative (Fig. 3).

A noticeable characteristic of the flows was the generation of vigorous boils arising periodically from the neighborhood of the foot of the vegetation boundary without accompanying horizontal large eddies along the boundary, which are often observed and studied. Fig. 4 is a sketch of a flow pattern of water surface with boils, that was illustrated from several observation photographs for water surfaces of flow: The boils strongly extended over the water surface of the non-vegetation area in a diagonal elliptic shape to give intensive secondary flows into the vegetation area and into the high velocity area of the opposite side. Visual measurements for boil generation

in Case 2 showed that the time for 100 boils to pass through the measuring site was 364 seconds, i.e. the average period for boil generation was 3.64 seconds. Hence, the mean boil length was estimated at about 3.2 m using the mean flow velocity. After one boil passed downstream, a low velocity fluid with an arm-like pattern was pulled from the vegetation area into the main flow area. When an upstream boil with a mean flow velocity overtook the low velocity fluid, formation of small scale eddies were seen along the front of the arm. The arm-like pattern sometimes seemed to rotate, like a horizontal eddy when visualized using aluminum powder. This was conspicuous in Case 2, which has a thinner vegetation density. The transverse surface flow toward the opposite side of the vegetation area, i.e. to the left bank, which was just the surface boundary flow of boils, seemed to sink at the position 30 – 40 cm from the left concrete wall. Pumice stones brought from the bed converged near the sinking points to make a wavy line with wavelengths depending on the boil length.

Individual model reeds did not swing so severely for the flow during the experiment, but fairly vigorous swings of model reeds were seen at the place where the surface flow went into the vegetation area. The flow velocity was very small, and no reverse flow was observed in the vegetation area. However, a relatively strong transverse flow to enter the vegetation area and a weak transverse flow pulled from the vegetation area appeared alternately to make periodical change of density of aluminum powder with a wavelength of approximate 5 m. The wave pattern visualized by the aluminum powder in the vegetation area did not change from a constant form, although boils passed downstream.

Mean Flow Velocity

Figs. 5(a) and 5(b) show results of measurements for the first time of transverse distributions for time-averaged flow velocity in the downstream direction in Case 1 and Case 2, respectively. Symbols and distances in the figures correspond to the specific heights of measurements points shown in Fig. 1(c). The figures show that the intensity of lateral velocity gradient $\partial \bar{u} / \partial y$ at the vegetation boundary and the position of the reflection point of velocity distribution curve are different to each other depending on the difference in vegetation density: In Case 1, the velocity gradient at the vegetation boundary is steep and the reflection point is outside the boundary, while in Case 2 the gradient is gentle and the reflection point is in the vegetation area. Moreover, the fact is worth noting that the velocity distributions are flat near the outer portion of 10 – 40 cm in Case 1, or 10 – 30 cm in Case 2, separate from the vegetation boundary.

Figs. 6(a) and 6(b) show vertical profiles of time-averaged velocity in the downstream direction in Case 1 and Case 2, respectively. Symbols and distances in the figures correspond to the vertical traverse lines a - k shown in Fig. 1(c). As shown in the figures, the velocity of the inner flow in the vegetation area (traverse lines h – k) have an almost constant value vertically and transversely. On the other hand, in the non-vegetation area (traverse lines a – g), the profiles have a peculiar distribution with a peak near the 20 - 30 cm upper position from the bed, differing largely from the normal logarithmic distribution. The closer a place is to the vegetation boundary, the more the peculiarity of velocity profile at the place tends to increase. The velocity gradient in Case 1 with a high vegetation density is steeper than that in the Case 2.

Figs. 7(a), 7(b) express vertical distributions of the transverse component of the flow velocity along traverse lines a - k in Case 1 and Case 2, respectively. In both cases, obvious stream lines of secondary flows are difficult to find because of complex patterns in the profiles. However, a transverse surface flow towards the left bank away from the vegetation boundary and a partial spiral flow are confirmed in Case 1, with a superposed dominant mean lateral flow from the left bank to the right bank. Further, in Case 2, development of a spiral flow with

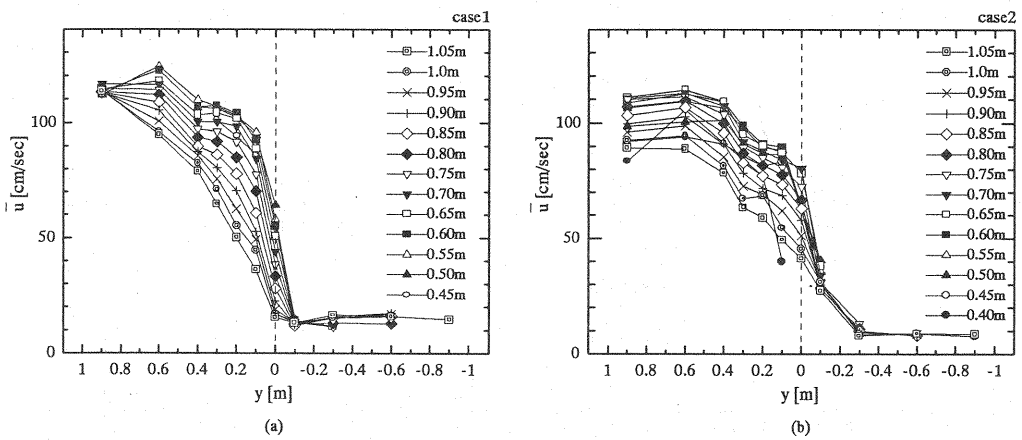

Fig. 5 Transverse distributions for time-averaged flow velocity in the downstream direction, (a) Case 1, (b) Case 2.

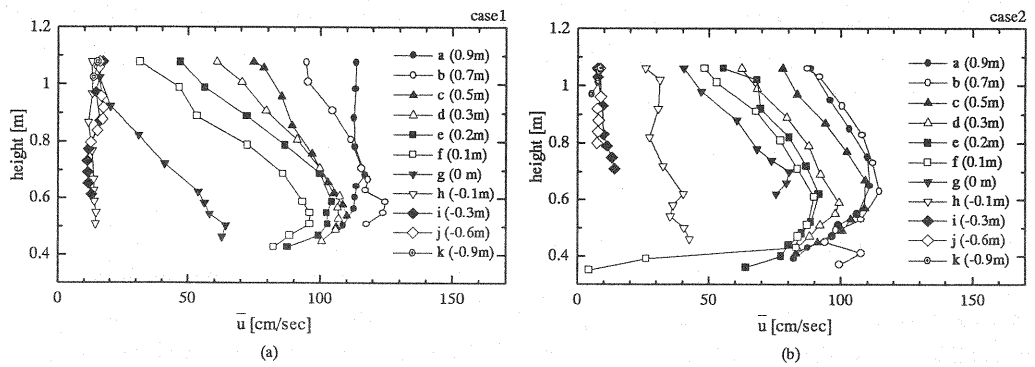

Fig. 6 Vertical profiles of time-averaged velocity in the downstream direction, (a) Case 1, (b) Case 2.

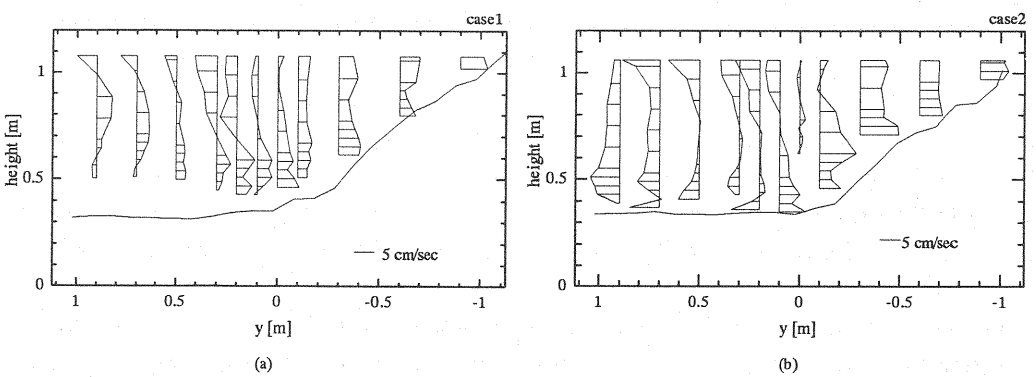

Fig. 7 Vertical distributions of the transverse component of the flow velocity, (a) Case 1, (b) Case 2.

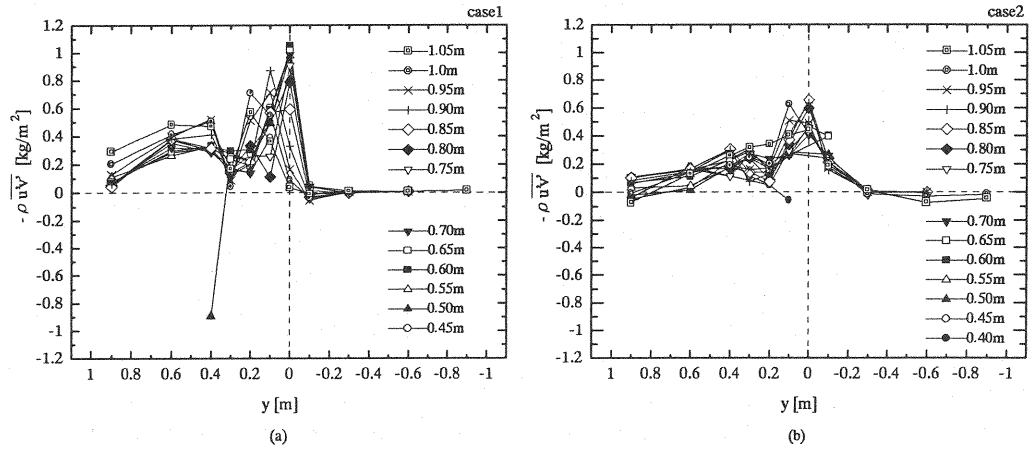

Fig. 8 Transverse distributions of lateral Reynolds stress at each depth, (a) Case 1, (b) Case 2.

accompanying divergent flow toward both sides is found near the vegetation boundary. These transverse flows may be generated by the rising strong boils. A stable structure for the secondary flows or spiral flows was not observed because of the shortage of measuring time for the flow velocity in these experiments.

Reynolds Stresses

From the data of turbulent velocity components u', v' and w' in the x, y and z directions, lateral Reynolds stress ($-\rho\overline{u'v'}$) and horizontal Reynolds stress ($-\rho\overline{u'w'}$) were obtained. Figs. 8(a), 8(b) show the transverse distributions of ($-\rho\overline{u'v'}$) in Case 1 and Case 2, respectively. Symbols and distances in the figures indicate the vertical specific heights of the measurement points. For both cases, the maximum shearing stress arises just on the vegetation boundary if the specific height of the point is under 80 cm. However, the position of maximum shearing stress tends to shift within the non-vegetation area if the specific height of the point is greater than 80 cm. The transverse change of lateral shearing stress shows that the stress decreases in the portion of 10 – 30 cm from the vegetation boundary and again increases toward the left bank. This corresponds to the fact that the transverse velocity distribution has a flat form in the portion of 10 – 40 cm (Case 1), or 10 – 30 cm (Case 2) from the boundary, where the velocity gradient $\partial\overline{u}/\partial y$ gets close to null.

Figs. 9(a), 9(b) indicate the vertical distributions of horizontal Reynolds stress ($-\rho\overline{u'w'}$) in Case 1 and Case 2, respectively. Symbols and distances in the figures show the traverse lines a - k in Fig.2 and their y-coordinates. For both cases, the sign of Reynolds stress changes from positive to negative bounded by the position of the 50 – 60 cm specific height; the shearing stress becomes negative between the bounded point and water surface, corresponding to the appearance of negative $\partial\overline{u}/\partial z$ in the area and the occurrence of the maximum velocity at the bounded point. Near the bottom, the shearing stress would have large positive values, but the shearing stress was not obtained in these experiments, because it was impossible to measure the velocities within a space of several centimeters above the bottom owing to existence of dunes in the movable bed experiments.

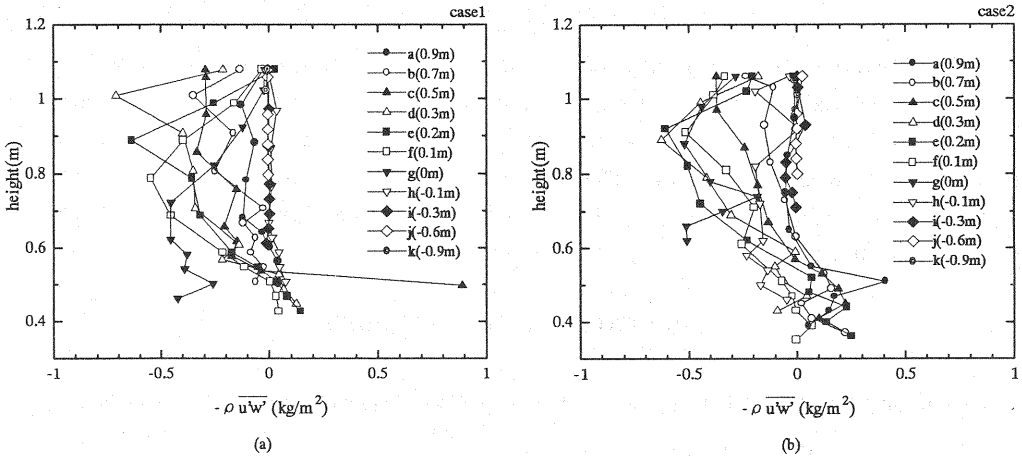

Fig. 9 Vertical profiles of horizontal Reynolds stress, (a) Case 1, (b) Case 2.

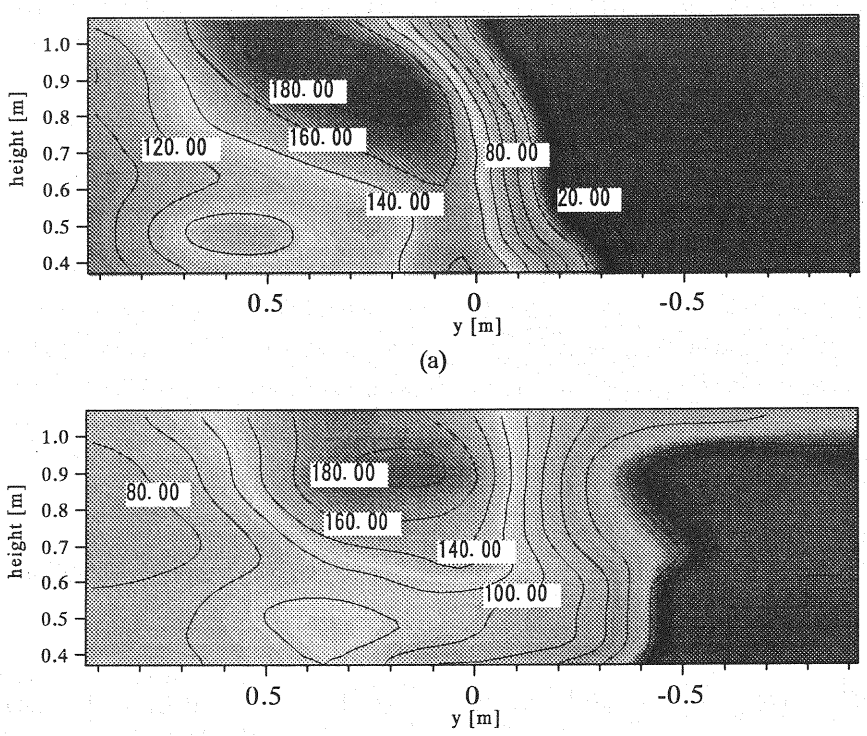

Fig.10 Turbulent energy contour lines in the observing cross section, (a) Case 1, (b) Case 2.

Turbulent Energy

In figures 10(a) and 10(b), cross sectional distributions of turbulent energy are shown with contour lines in Case 1 and Case 2, respectively. A ridge line of the contour map, which can be seen especially in Case 1 clearly, suggests the generation and transportation of boils rising to the water surface from the foot of the vegetation boundary. In Case 2, boils seem to rise to the water surface from a point in the upper third of the water depth from the bottom on the vegetation boundary. The difference between the two cases would be the difference in appearance position of the reflection point in the transverse distribution of mean flow velocity (Figs. 5(a), 5(b)), which may be caused by the difference in the vegetation density.

EQUILIBRIUM OF THE FLUID FORCES

The following equation is used to analyze the equilibrium relationship of the fluid forces in the x-direction.

$$-\rho\int_{\zeta}^{H}\left(\overline{uv}\right)_{y=0}dz=\rho gAI_m+\rho\int_{\zeta}^{H}\left(\overline{u'v'}\right)_{y=0}dz+\rho\int_{0}^{B}\left(\overline{u'w'}\right)_{z=\zeta}dy$$

where ρ = the density of water; H = the water surface height; ζ = the bed surface height; A = the cross sectional area in non-vegetation area; $I_m = -\partial(H+\beta U^2/2g)/\partial x$ = the momentum gradient; B = the channel width of the non-vegetation area; β = the momentum correction factor; U = the cross sectional mean flow velocity; $\overline{u}$, $\overline{v}$ = the time averaged flow velocity component in x- and y- direction at any point, respectively; u', v' = the perturbations from u and v, respectively; w' = the turbulent velocity component in z-direction.

The term on the left side of the equation indicates the force caused by momentum transport by transverse secondary flows through the vegetation boundary. The first, second and third terms on the right side of the equation indicate the downstream component of gravitational force, the summation of lateral Reynolds stress acting on the vegetation boundary and the summation of bottom shearing stress, respectively. Here, the bottom shearing stress is estimated by substituting each observed value of the other three terms into the above equation, because the measurement of bottom shearing stress was actually impossible in the experiments. Table 2 shows the results of a reverse calculation of the bottom friction factor. These values of the friction factor are approximately equal to the values ($C_f = 0.01$) that were evaluated in previous bank erosion experiments (8) carried out using a bare soil bank and the same experimental facilities as this study. Therefore, the fact that the

Table 2 Equilibrium relationship of the fluid forces in the x direction (unit: kgf/m)

Case	ρgAI_m	$\rho\int_{\zeta}^{H}\left(\overline{uv}\right)_{y=0}dz$	$-\rho\int_{\zeta}^{H}\left(\overline{u'v'}\right)_{y=0}dz$	Bottom Frictional Force	Bottom Friction Factor
Case 1	2.28	- 0.79 (35%)	- 0.40 (17%)	- 1.09 (48%)	0.0122
Case 2	1.82	- 0.48 (27%)	- 0.37 (20%)	- 2.24 (53%)	0.0119

observed value for each term listed in the Table 2 was generally true would have been proved, even though it was done with the indirect way. Each ratio of the momentum transport by the secondary flow, the lateral Reynolds stress acting on the vegetation boundary and the bottom shearing stress to all the resistant forces has a percentage value in the corresponding column of Table 2. From the results the lateral Reynolds stress in Case 2 show a higher ratio than that in Case 1. This may be because of the ease of Case 2 in realizing the momentum mixing on the vegetation boundary.

SUMMARY AND REMARKS

(1) Large scale horizontal eddies that are generally known to develop along the vegetation boundary were not found in a flow field having a comparatively deep water depth with high vegetation density on the bank. Rather, the periodical generation of vigorous boils predominated. The boils cause strong transverse secondary flows to affect the velocity fields in various characteristic ways.

(2) Strongly deformed velocity distributions of the main flow, such as the maximum velocity, arose at one third water depth from the bed in the flow field near the vegetation boundary, which may be caused by transport of fluid mass with a very low speed i.e. boils from the bottom vicinity of the vegetation boundary. In the case of high vegetation density of the three-dimensional numerical simulations performed by Nezu (4), the result also shows a fall of the position of the maximum flow velocity.

(3) A transverse distributing form of the main flow velocity in the non-vegetation area had a partially constricted or flattened shape near the vegetation boundary. According to the results of a numerical simulation by Shimizu (6), which was designed to include growth of secondary flow, the same constriction of transverse velocity distribution can be found in the area where the secondary flow rises and makes cells within the cross section. Hence, we presume that the constriction in the transverse velocity distribution would be caused by the action of boils.

(4) The influence of boils extends to the distribution of lateral Reynolds stress; the distribution undulates to cope with the change in lateral velocity gradient at the same place where the constriction of velocity distribution occurs.

(5) The distribution of turbulent intensity shows some relationships with the loci of rising boils and has a maximum value near the water surface. From a comparison of both case experiments, the location of the source of boils was different depending on the difference in vegetation density.

(6) The resistance force due to each component of lateral Reynolds stress on the vegetation boundary, the momentum transport by secondary flow and the bottom shearing force increases in this order. The lateral Reynolds stress in Case 2 has a larger value than in Case 1, which may be caused by the difference in ease of realizing the momentum mixing on the vegetation boundary.

REFERENCES

1. Asai, S., K. Hasegawa, Y. Watanabe and S. Kanetaka : An experimental study on bank erosion and accumulation in a large-scale experimental channel with reeds, Proceedings of Hokkaido Chapter of the JSCE, No.52(B), pp.194 - 199, 1996 (in Japanese).
2. Ikeda, Y. : Evaluation of sediment tractive force and sediment motion, 3.3 ; Influence of vegetation on channel change, 3.4 : Vegetation in rivers and channel morphology, Document No.1, River Environments Management

Foundation, pp.79 - 100, 1995 (in Japanese).
3. Kanetaka, S., Y. Watanabe, K. Hasegawa and Y. Kameta : Experimental study on volcanic ash soil bank erosion using large scale flume, Proceedings of Hydraulic Engineering, Vol.37, JSCE, pp.631 - 636, 1993 (in Japanese).
4. Nezu, I., Dan Naot and H. Nakagawa : Numerical simulation of 3-D velocity distribution in open –channel flows with vegetation, Annual Journal of Hydraulic Engineering, Vol.39, JSCE, pp.507 - 512, 1995 (in Japanese).
5. Okabe, K. : Flows passing through vegetation area, 3.1 ; Flows in a river channel with vegetation, 3.2 : Vegetation in rivers and channel morphology, Document No.1, Foundation of River Environments Management, pp.61 - 79, 1995 (in Japanese).
6. Shimizu, Y., T. Tsujimoto and H. Nakagawa : Numerical study on fully- developed turbulent flow in vegetated and non-vegetated zones in a cross-section of open channel, Proceedings of Hydraulic Engineering, Vol.36, JSCE, pp.265-272, 1992 (in Japanese).
7. Tsujimoto,T. : Flow hydraulics of vegetation rivers, Text of the 27th Summer School on Hydraulic Engineering in Course A, the Committee of Hydraulics, JSCE, pp.A-5-1 – A-5-22, 1991 (in Japanese).
8. Tsujimoto, T. and T. Kitamura : Experimental study on mechanism of transverse mixing in open-channel flow with longitudinal zone of vegetation along side wall, Jour. of Hydraulic, Coastal and Environmental Engineering, No.491/II-27, JSCE, pp.61 - 70, 1994 (in Japanese).
9. Watanabe, Y. : Vegetation trees and hydraulics, Text of the 31st Summer School on Hydraulic Engineering in Course A, the Committee of Hydraulics, JSCE, pp.A-9-1 – A-9-19, 1991 (in Japanese).

APPENDIX - NOTATION

The following symbols are used in this paper:

- A = cross sectional area in non-vegetation area;
- B = channel width of the non-vegetation area;
- C_f = friction factor of the bed;
- g = gravitational acceleration;
- H = water surface height measured from the bottom of the concrete channel;
- I_m = momentum gradient;
- $\overline{u}$ = time averaged flow velocity component in x-direction at any point;
- u' = turbulent velocity component in x-direction;
- U = cross sectional mean flow velocity;
- $\overline{v}$ = time averaged flow velocity component in y-direction;
- v' = turbulent velocity component in y-direction;
- w' = turbulent velocity component in z-direction;
- x = horizontal axis in the downstream direction;
- y = horizontal axis perpendicular to the x-axis;
- z = vertical axis taken from the bottom of the concrete channel;
- β = momentum correction factor;
- ζ = bed surface height measured from the bottom of the concrete channel; and
- ρ = density of water.

(Received August 31, 1998 ; revised July 2, 1999)